Proceedings World Geothermal Congress 2015
Melbourne, Australia, 19-25 April 2015

Hydrothermal Fluid Flow in a Structurally-controlled Basin, Ngakuru Graben, Taupo Rift, New Zealand

Warwick Kissling, Andrew Rae, Pilar Villamor and Susan Ellis

GNS Science, 1 Fairway Drive, Avalon 5010, New Zealand

w.kissling@gns.cri.nz

Keywords: *Ngakuru Graben, geothermal systems, silica sinter, hydrothermal alteration, fluid flow, modelling, TOUGH2*

ABSTRACT

The Ngakuru Graben lies in the northern Taupo Rift, New Zealand and hosts a number of major geothermal areas on its western and eastern margins – including Te Kopia, Waikite, Orakeikorako, Atiamuri and Horohoro. As well as these active geothermal systems, areas of extinct hydrothermal activity (i.e. silica sinter, hydrothermal eruption deposits and hydrothermally-altered tephras and lake sediments) are also found at the margins of the graben, including its northern and southern terminations. The graben contains four major active faults (or fault systems) – the Ngakuru, Maleme, Whirinaki and Paeroa. These not only define the graben structurally but play host to its hydrological system which, because of the deep interconnectedness of the faults, can behave in a complex way when there are significant, sudden changes in the fault permeabilities. Such changes are expected to have implications for the location and longevity of past geothermal activity in the graben, as interpreted from fossil sinter formations and other manifestations.

A numerical model of this system has been developed using the fluid flow code TOUGH2. The model represents the major geological features of the area and a recently inferred deep heat source to the east of the Paeroa fault. We explore models where there are major perturbations to the permeabilities of the faults. An increase in fault permeability is assumed to be associated with a fault rupture, while a permeability reduction to 'background' values can occur as a result of (unmodelled) chemical or geological processes. The key result from the modelling is that the flows in an inter-connected system of faults are complicated, and fluid pathways can be altered by changes in the fault permeabilities. More specifically, despite significant changes in the flows immediately following a rupture, even large increases in fault permeabilities do not lead to major changes such as the cutoff or reversal of flow in the faults on ~100 year timescales. Conversely, we identify a model where a reduction in fault permeability leads to drastic changes in the flows, and these have important consequences for the fossil sinter deposits found at various locations within the Ngakuru graben.

1. INTRODUCTION

The Taupo Rift is geologically one of the "hottest" rifts in the world, with high crustal heat flow (~ 700 mW/m^2; Bibby et al. 1995), high extension rates (up to 12 mm/yr, Wallace et al., 2004), and high silicic eruption rates (e.g., 12.8 km^3 Ka^{-1}; Wilson et al., 2009) and volumes (>35 km^3; Wilson et al., 2009). In this geological environment, numerous active geological processes are contributing to defining the characteristics and evolution of geothermal systems located within the rift.

The Ngakuru Graben in the northern Taupo Rift, has areas of current and fossil geothermal activity located along the basin margins. Geothermal systems occur on the eastern and western margins at Te Kopia, Waikite, Ngapouri, Orakeikorako, Atiamuri and Horohoro. Fossil geothermal areas, in the form of deposits of silica sinter and hydrothermal eruption breccia, as well as hydrothermally-altered tephras and lake sediments are located elsewhere on the graben margins. The coexistence of active and extinct hydrothermal activity among a dense and complex active fault network, and the proximity to large active and extinct silicic volcanic centres, provides a unique opportunity to gain insights into the evolution of geothermal activity in a structurally controlled basin. Both the active and fossil geothermal areas and their spatial relationship to fault structures are the subject of this paper. In particular, we are concerned with understanding the role of faults providing the permeability that gives rise to these geothermal areas in the Ngakuru graben. We address important questions as to what controls the flow of fluid to the surface, why are surface expressions mainly restricted to the basin margins, and how can we explain their apparent ephemeral nature.

A hydrological model of the graben has been developed using TOUGH2, which will address these questions and test the influence of both fault architecture and the rate of tectonic activity on hydrothermal activity. The model represents the major geological features of the area on a 30 km wide 2-D northwest-southeast cross-section of the graben that extends to a depth of 7 km. This depth corresponds to the depth where ductile processes are expected to reduce the permeability to a level too low to support convective fluid flow (Bryan et al., 1999; Bibby et al., 1995). The model includes four major faults for which good estimates of average slip rates and other properties are available – the Ngakuru, Maleme, Whirinaki and Paeroa faults. The permeabilities of these faults are estimated from their slip rates, and permeabilities elsewhere in the model are drawn from our experience with regional-scale models of the area (Kissling and Weir, 2005).

2. GEOLOGICAL AND GEOTHERMAL SETTING OF THE NGAKURU GRABEN

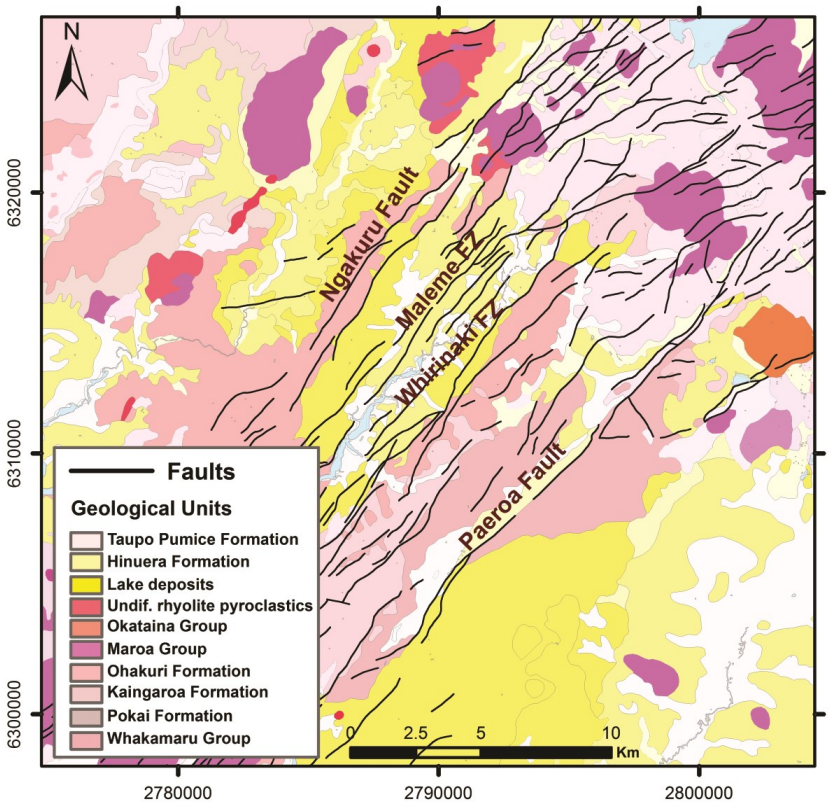

Figure 1: Geological map of the Ngakuru Graben (Leonard et al., 2010).

The Ngakuru Graben lies in the northern Taupo Rift (Acocella et al., 2003), a tectonic structure within the Taupo Volcanic Zone (TVZ); the volcanic arc associated with the Hikurangi subduction margin (Wilson et al., 1995). Within the Ngakuru Graben, rift extension is ~8 mm/yr (Villamor and Berryman, 2001; Wallace et al., 2004), and the structural fabric is characterised by northeast-trending normal faults, with opposing northwest- and southeast-facing fault dips defining a central rift axis (Rowland and Sibson. 2001). The graben is bounded by the active eastern Paeroa and western Ngakuru faults (Figure 1), is only ~ 15 km wide and has the densest surface fault network of the whole Taupo Rift (100 to 50 m spacing).

Surface geology of the graben is dominated by rhyolitic volcanic and volcaniclastic rocks and lacustrine sediments (Figure 1; Leonard et al., 2010). The Paeroa Ignimbrite (Whakamaru-group, 320-340 ka; Wilson et al., 1986) is the oldest unit mapped in the basin and occurs in its southern and southeastern parts (Figure 1) abutting against and offset by the Paeroa Fault. Kapenga Rhyolite domes (Maroa Group) occur along the northern and northeastern graben boundary. The Ohakuri Formation (ca. 240 ka; Gravley et al., 2007) is a non-welded pumice-crystal tuff that occurs as fault-parallel ridges within the basin. Kaingaroa Ignimbrite (230 ka; Houghton et al., 1995) is restricted to the southern part of the basin, west of the Paeroa Ignimbrite. Lake sediments of the Tauranga Group (Leonard et al., 2010) overlie the ignimbrites. These are a sequence of finely stratified siltstones, vitric and pumice tuffs, diatomites, sandstones and conglomerates (Brathwaite, 2007) that occur between blocks of uplifted Ohakuri Formation. Earthquake Flat rhyolitic pyroclastic flows and air fall deposits (64 ka; Wilson et al., 1992) outcrop in the northeastern parts of the basin. Most recently, Quaternary surface alluvium (that includes Taupo Pumice alluvium) is distributed along structurally-controlled valley floors.

Areas of surface geothermal activity within the graben currently occur at Waikite, Ngapouri, Te Kopia, Orakeikorako, Atiamuri and Horohoro, and are highlighted as areas of anomalously low electrical resistivity (i.e., <20 Ωm; Figure 2; Stagpoole and Bibby, 1998). All these areas are confined to the western and eastern basin margins, with an apparent focus of geothermal activity associated with the eastern Paeroa fault, at Waikite, Orakeikorako, Te Kopia and Ngapouri.

Surface mapping of the basin by previous workers (e.g., Brathwaite, 2007, and references therein) has identified sites of extinct geothermal activity (e.g., Ohakuri), in the form of silica sinter deposits, hydrothermal alteration (e.g., zeolite-altered lake sediments) and hydrothermal eruption breccias (Figure 2). Many of these sites occur above or on the margins of electrically conductive areas (Figure 2), and as with active geothermal sites, all are located marginal to the structural basin (Figure 2). Radiometric dating (^{14}C) of organic material trapped in sinter sampled from various sites shows that hydrothermal activity has been ongoing on the margins of the Ngakuru Graben for at least the last 34 ± 0.5 ka.

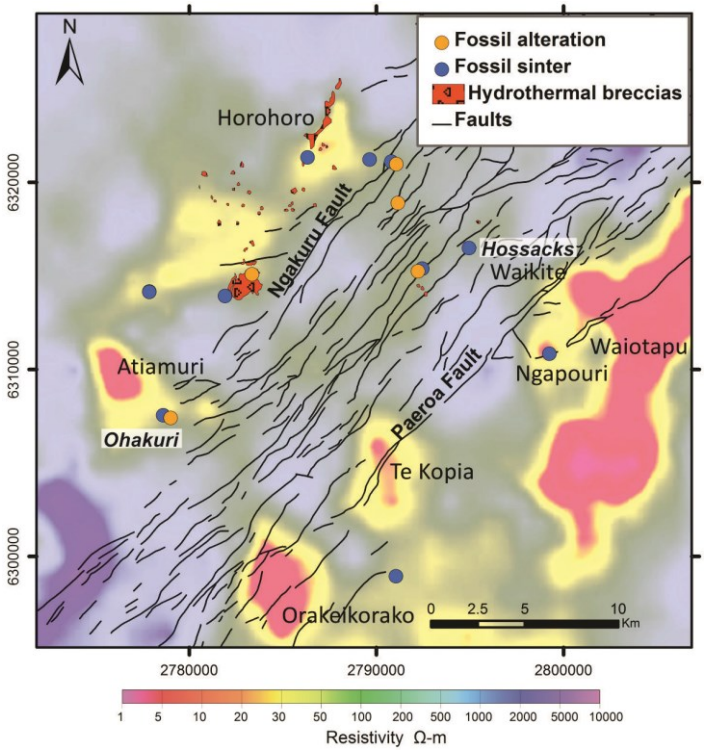

Figure 2: Electrical resistivity map of the Ngakuru Graben (detail from Stagpoole and Bibby, 1998; nominal array spacing 500 m) with local active geothermal systems indicated, along with sites of extinct hydrothermal activity in the form of silica sinter deposits, hydrothermal alteration and eruption breccias. Active faults are taken from Leonard et al. (2010).

An inferred deep heat source below the south-eastern margin of the graben is based on information from an array of broadband magnetotelluric (MT) measurements at the south-eastern margin of the TVZ (Heise et al., 2010; Bertrand et al., 2012). Most of this array was located south-west of the Ngakuru Graben, but along its northern-most edge images of the region beneath the southern Ngakuru Graben and the Te Kopia geothermal area were obtained. Despite the sparse data coverage, narrow, vertical zones of low resistivity that are separated by broad zones of higher resistivity at depths of 3-7 km are interpreted as hydrothermal convection plumes. Beneath these plumes and generally offset from them are broad deep zones of low resistivity at ca. 7-8 km depth. These are proposed to represent regions of partial melt (Bertrand et al., 2012). The MT profiles in the southern Ngakuru Graben show a deep region of low resistivity offset ca. 5 km to the east of the Te Kopia geothermal area and the surface expression of the Paeroa Fault; it extends over ca. 8 km horizontally eastwards.

3. PREVIOUS HYDROLOGICAL MODELS OF THE NGAKURU GRABEN

Dempsey et al. (2013) used a combined hydrological-mechanical numerical model to investigate the near-field effects from a fault on the Te Kopia geothermal system, which is located astride the Paeroa Fault (Figure 2). In their model they assumed that the Paeroa Fault acted as a barrier to fluid flow between earthquake ruptures, and applied a circular region of elevated heat and fluid flow beneath the fault to represent Te Kopia geothermal system. The fault acted to partition the fluid flow on the hanging wall and footwall blocks, with the magnitude of the partitioning dependent on the location of the deep heat source. This model configuration was then used to explore the effect of coseismic perturbations to pore pressure and permeability. When the fault permeability was suddenly increased, mass and heat flows at the surface increased for a short time by over 200%, but then decayed rapidly back to base values over time periods of days. While the short-term behaviour was dominated by changes in pore-pressure, the longer term changes in flows were due to the increase in permeability. In this study, although we use a different model configuration, we further pursue the effects of coseismic permeability changes in the context of the interconnected fault system of the Ngakuru Graben.

4. MODEL DESCRIPTION

4.1 Fluid Flow Modelling Code

For the models presented in this paper the original version of TOUGH2 (Pruess, 1991) does not have a sufficient working range of temperature and pressure (up to 350°C and 800 bar) so we use an extended version (Kissling, 1995) which uses supercritical fluid properties (to 2000°C and 3000 bar) derived from the NIST formulation (Haar, Gallagher and Kell, 1984). TOUGH2 is a fully implicit integrated finite difference code which solves the (highly nonlinear) time dependent equations for mass and energy conservation in a porous medium, together with appropriate constitutive relationships for the density, enthalpy and viscosity of liquid water and steam. The transport of fluid is described by Darcy's law. These calculations yield the mass and heat flows, and the pressure and temperature distributions within the model domain.

4.2 Model Setup

The TOUGH2 model domain covering the Ngakuru Graben is 30 km wide and 7 km deep, and represents a 2D northwest-southeast section across the central graben (Figure 1). The graben itself is approximately 11 km wide at the surface, narrowing to about 3 km at the base of the model. It is defined to the northwest and southeast respectively by the Ngakuru and Paeroa faults (e.g., Rowland and Sibson, 2001), and two other central faults, the Maleme and the Whirinaki, are also represented within the graben. The implementation of the faults in the model is discussed in section 3.3.

The base of the model is assumed to mark the approximate depth at which permeability starts to decrease due to the onset of ductile processes. Although the seismicity cut-off depth marking onset of ductile behaviour in the TVZ occurs on average at about 6-7 km (Bryan et al., 1999), the brittle-ductile depth in geothermal fields is likely to vary spatially depending on presence of partial melt zones and the interaction with local fluid flow along faults (e.g., Matsushima and Okubo, 2003; Kissling et al., 2009). Since fluid downflow occurs over most of the Ngakuru Graben, the average geothermal gradient may be lower than in other parts of the TVZ, while that directly above zones of partial melt (e.g., on the eastern margin) will be higher. We do not explore this complexity here (cf. Kissling et al., 2009), but instead assume an average depth of 7 km to which fluid circulation dominates. This allows us to isolate the sensitivity of the model to fault-permeability perturbations. A future study will explore the links between such perturbations, strain-rates, and variations in brittle vs. ductile behavior and its effect on permeability and fluid flow in this region.

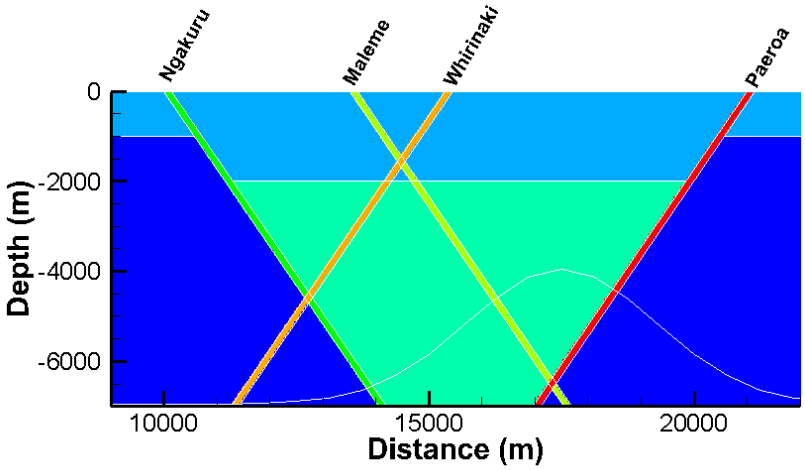

Figure 3: Close up of the central 13 km of the model. The Ngakuru Graben is centered in the model domain and is cut by four major faults, as labeled. The colours indicate the seven different rock types in the model. The faults are each assigned a distinct rock type and for the major units light blue indicates the 'shallow infill', green the 'deep infill' and dark blue the low permeability exterior unit. The 'Gaussian' curve shows the location distribution of the deep heat source applied at the lower boundary of the model.

The model contains three major geological units and four distinct rock types for the faults, as listed in Table 1 and shown in Figure 3. The upper 1 km exterior to the graben, and the upper 2 km within it contain a shallow infill unit consisting of moderate-permeability uncompacted volcanics. Deeper within the graben a lower permeability deep infill unit extends to the base of the model. Finally, exterior to the graben but deeper than 1 km, a very low permeability 'exterior' unit is used. As noted in section 2.2, we assume that all rocks remain permeable above 7 km, but below this the permeability is too low to support convective fluid flow. Table 1 also gives permeabilities for these units – they are assumed to have fixed isotropic permeabilities (i.e. horizontal component equal to vertical component) which remain unchanged during the simulations. All rocks are assumed to have a porosity of 0.1, thermal conductivity of 2 W/m/K, specific heat capacity of 1000 J/kg/K and a density of 2650 kg/m^3.

Table 1: Major rock types and associated permeabilities

Rock Type	Permeability (mD)
Shallow Infill/volcanics	10
Deep Infill	1
Exterior	0.001
Faults	see Table 2, section 3.3

The TOUGH2 model we use to represent the graben contains approximately 30,000 elements. The elements are varied in size to provide higher resolution within the faults while they remain larger elsewhere in the domain where lower resolution is sufficient. The mesh design ensures that no two neighbouring elements differ in size by more than a factor of two. The element sizes range from 500 m at the lateral boundaries to ~30 m (actually $500/2^4$ m = 31.25 m) within the faults. This has allowed us to represent faults of more realistic width (nominally 150 m ≡ 5 model elements), something which is not practical with a uniform mesh because of the prohibitive number of elements involved.

The upper boundary (i.e., the ground surface) is modelled by a fully liquid-saturated block held at 1 bar pressure and 20°C. As discussed by Kissling and Weir (2005), this adequately represents the situation in the TVZ/Taupo Rift where only a small fraction of the rainfall is needed to provide the recharge for the geothermal systems. At the lower boundary of the model we apply a constant background heat source of 50 mW/m^2 , sufficient to support a geophysical temperature gradient of 25°C/km. An additional geothermal heat source (shown in Figure 3) is discussed in section 2.2 and used to represent a remnant heat source thought to exist below the graben (Heise et al., 2010; Bertrand et al., 2012). This is centered at X=19 km in the model domain, and has a 'Gaussian' profile with a peak heat flux of 1000 mW/m^2 (comparable to the average heat flux in the TVZ, Bibby et. al., 1995) and a full width at half height of approximately 3.3 km.

Initial conditions for the model are discussed in section 4.1.

4.3 Modelling Faults and Fault Permeabilities

In this paper we examine two extremes of fault behaviour – the first where the permeability is enhanced to a level significantly above its long-term average value, and the second where the permeability is reduced sufficiently so that it no longer plays a significant part in the regional scale hydrology. These we associate with the faults either rupturing (enhancing the permeability), or becoming sealed (reducing the permeability) through hydrothermal alteration. A very simple approach is taken to modelling these processes – both the enhancement and reduction of permeability are assumed to occur instantaneously and throughout the fault in question. Normally, the permeability reduction due to sealing might be expected to decay roughly exponentially over yearly-decadal timescales (e.g. Ingebritsen and Manning (2010)), but this is difficult to implement in TOUGH2 and is deemed unnecessary for the present purpose.

Villamor and Berryman (2001) interpret that the numerous surface fault traces mapped in the graben merge at depth into seven major faults. Four of those faults have a stronger surface expression and accommodate most of the extension of the rift at this latitude. These faults are from east to west, the Paeroa, Whirinaki, Maleme and Ngakuru faults (Figures 1 and 3) and have slip rates of ~ 1.5, 0.7, 1.5 and 0.5 mm/yr, respectively (Table 2; Villamor and Berryman, 2001; Canora-Catalan, 2008; Berryman et al., 2008). The amount of co-seismic displacement and rupture recurrence for these faults has been derived from published and unpublished information and is shown in Table 2 (Stirling et al., 2012; Litchfield et al., 2013 and references therein). Deep subsurface expression of these faults is unknown and thus fault dips are uncertain. Based on a compilation of fault data from the Taupo Rift and other extensional areas, active faults in this area are assigned a dip of 60 ± 10º (Villamor and Berryman, 2001)

The major geological units in the model are cut by the four active faults described above, (Figure 3). These faults are assumed to have a fixed fault zone width (nominally 150 m), and a fixed dip angle of 60° to the base of the model. The finite-thickness fault zones are modelled with homogeneous, isotropic physical properties and have higher permeabilities than surrounding crust, representing the bulk effect of a permeable fault damage zone. The faults are represented identically in the model as permeable zones, 4-5 of the smallest (~30 m) model elements in width. Numerical experiments suggest that this degree of refinement is necessary to achieve adequate resolution of flow within a fault, which can often exhibit strong gradients cross-fault, or even internal circulation leading to reversals of flow direction. In these cases models with lower resolution (say only 1-2 elements) do not perform well and can suffer from poor convergence.

Within each fault, a uniform permeability is assigned, with the same values for the along-strike and cross-fault components. While there is little guidance as to the absolute values of the permeabilities, we found that values of ~100's mD behaved well in the numerical model and produced interesting behaviour that provides insight into the regional scale hydrology of the graben. The permeabilities we assigned initially were based on the time-averaged slip rates of the faults (see Table 2), which meant that the permeabilities on the Maleme and Paeroa faults were identical (and equal to our assumed highest permeability of 300 mD). However, these permeabilities produce a natural state where the predominant upflow occurs on the Maleme fault, and not on the (preferred) Paeroa, which we consider to be the more active of the two, given the geomorphic expression (the Paeroa has produced a ~ 300 m high scarp), large co-seismic displacement and an apparent focus for current hydrothermal activity. Numerical experiments showed that enhancing the permeability of the Paeroa by a small amount (300 mD- 320 mD) was sufficient to change the location of the main upflow to that fault.

As with the long-term averaged permeabilities, there is no real guide to the degree to which the fault permeabilities might change during the rupturing or sealing processes. We therefore assume that the effect of a fault rupture is to increase the fault permeability to 1000 mD, a value significantly above the permeabilities elsewhere in the model. In a similar way, when a fault becomes sealed we reduce the permeability to 1 mD, equal to that of the deep infill. In both cases, we track model evolution after these step changes for 100 years. This is shorter than the typical recurrence times for any of the faults and so will not affect the time-averaged permeabilities given in Table 2. It is also possibly typical of the average time between any major disruptions of the hydrological system due to fault movement or other geological process. We do not attempt to model the evolution of the hydrological system beyond this time.

Table 2: Fault properties (from Villamor and Berryman, 2001), and permeabilities assigned to each fault.

Fault	Time-averaged Rifting Rate (mm/year)	Recurrence Interval (years)	Displacement (m)	Permeability (mD)
Ngakuru	0.5	1000	1.2	100
Maleme	1.5	700	1.1	300
Whirinaki	0.7	2800	1.4	140
Paeroa	1.5	600	1.7	320

5. RESULTS

In this section, we discuss three separate aspects of the model described in section 3. Firstly, we examine in detail the initial state of the model, which will provide insight into the regional-scale hydrological system and set the scene for later sections of this paper. In the following sections, we describe perturbations of this system due to the sudden enhancement of the fault permeabilities (section 4.2), and, conversely, to their sudden sealing (section 4.3).

5.1 Initial State

The initial conditions for the model are set up as follows. Firstly, we begin with a 'warm hydrostatic' pressure distribution throughout the model, corresponding to a conductive temperature gradient of 25°C/km. This is then evolved using TOUGH2 for a period of 200,000 years, and results in cool water penetrating to the base of the graben (Figure 4), with downflows from the surface hosted by the Ngakuru, Maleme and Whirinaki faults, and the sole upflow occurring on the Paeroa fault. In addition, there is a smaller component of downflow from the surface through the lower (but still moderate) permeability shallow infill. This state, where the graben is filled with cool fluid and there is a single upflow, is typical of many of the models we have run, although the location the upflow can change depending on the particular fault permeabilities used. As mentioned in section 3.3, our choice of fault permeabilities here was made to ensure that the predominant upflow in the model occurs on the Paeroa fault.

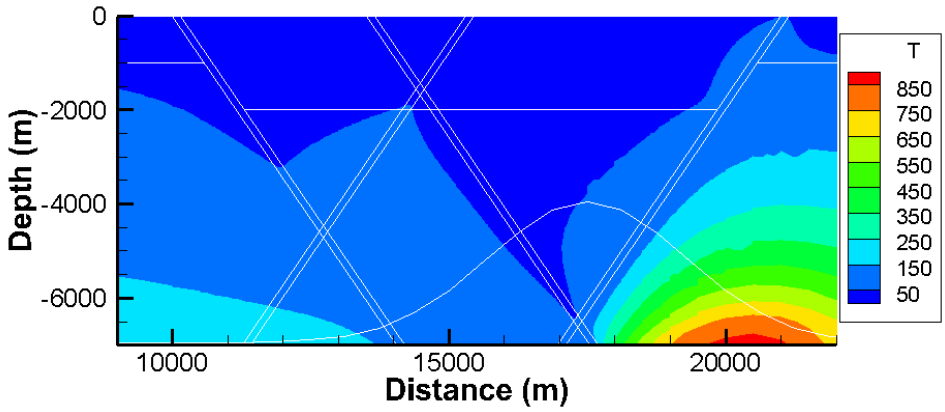

Figure 4: Initial temperature distribution used for the model. The Ngakuru, Maleme and Whirinaki faults support downflows, while the Paeroa fault supports the only upflow in the system, with a temperature of ~80°C. The remainder of the graben is filled with cool fluid from surface inflows from the remaining faults and from the moderate-permeability shallow infill region between them.

A summary of the flows within the graben/fault system for our chosen initial state are shown in Figure 5. At the surface, an upflow occurs in the Paeroa fault, with downflows occurring on the Ngakuru, Maleme and Whirinaki faults. The sum of these downflows is significantly less than the upflow in Paeroa, indicating that additional fluid is being added from the formation surrounding the faults. This occurs throughout the fault system - for example, the downflow in the Ngakuru fault above the Ngakuru-Whirinaki intersection (17×10^{-4} kg/m/s) is greater than the downflow in Ngakuru at the surface (3×10^{-4} kg/m/s). A similar inflow occurs to the Paeroa fault – this has an upflow of 103×10^{-4} kg/m/s just above the Maleme-Paeroa intersection, but at the surface the upflow is 126×10^{-4} kg/m/s. A surprising consequence of this inflow, and of the faults being hydraulically connected, is that there is a continuous and increasing flow through the fault system from the Ngakuru to the Paeroa fault with a 'traverse time' of ~100 kyr. This will not occur in the Ngakuru graben because many major fault movements would be expected to disrupt the flow during this period (see Table 2 for recurrence times). Nevertheless, it does give a feel for the magnitude of the inflows from the formation, which eventually comprise more than 60% of the total outflow at Paeroa. Overall, the model is very close to having a perfect mass balance. The outflow at Paeroa (126×10^{-4} kg/m/s) is balanced by the inflows in the other faults (46×10^{-4} kg/m/s), with the remaining fluid ($\sim80\times10^{-4}$ kg/m/s) entering the system at the surface through the surrounding shallow infill, mostly between the Whirinaki and Paeroa faults.

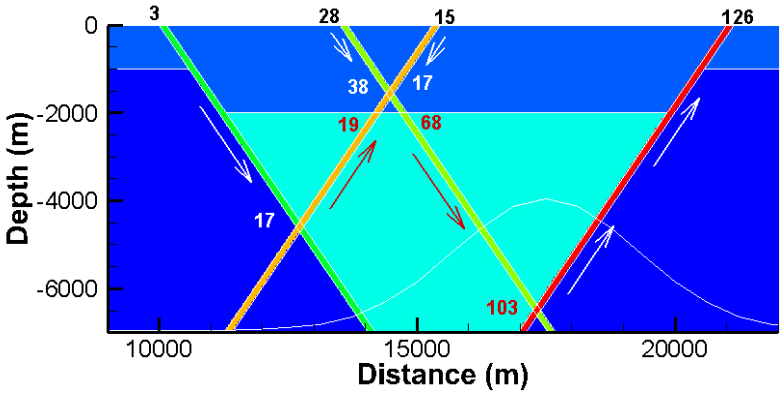

Figure 5: Summary of initial state flows in the model. The flows are given in units of 10^{-4} kg/m/s and the arrows indicate the direction of flow.

5.2 Effect of Fault Ruptures

In this section we examine how permeability-increasing ruptures on each of the four major faults affect the Ngakuru hydrological system, and in particular how they affect the flows through these faults which give rise to geothermal activity at the surface within the graben.

Table 4 summarises the changes in flow rates at the ground surface through each of the faults as a result of the fault ruptures. The left-most column lists which of the four faults has been ruptured, and the entries in the row following give the associated 'flow ratios', which express the ratio of the post-rupture to pre-rupture ground surface flow rates. This is a useful means of expressing changes in the flows because ratios which differ greatly from 1.0 imply large changes and are immediately apparent, regardless of the actual magnitude of the flow. Further, a positive flow ratio indicates that the flow direction stays the same, while a negative ratio shows a change of flow direction has occurred. The pre-rupture flow rates at the ground surface are given in section 4.1 and are also shown above each of the faults on Figure 5. Each of the four main columns in the table lists the flow ratios on each fault for a very early time (0.001 years) and at the end of the simulations (100 years).

The diagonal (yellow) cells give the flow ratios for the ruptured faults. At 0.001 years these are close to the post-rupture to pre-rupture permeability ratios – respectively 10, 3.2, 7.1 and 3.1 for the Ngakuru, Maleme, Whirinaki and Paeroa faults. This 'linear' response is not surprising, as our modelling uses the linear Darcy relationship between permeability and flow. We take no account of poro-elastic effects that might occur during fault rupture and which could give a nonlinear response to the permeability change. The corresponding 'off-diagonal' entries at this early time are all identically 1.0, because there has not yet been sufficient time for the flows to propagate through the fault system. We note also that the flow ratios are all positive, showing that the fault ruptures have not induced any flow reversals in the system at this time – flows that were initially downflows remain so, and the dominant upflow on the Paeroa fault remains an upflow.

A different flow regime has developed by 100 years. By this time the flow ratios show that the fault ruptures have induced more widespread effects of greater magnitude in the surface flows from the faults. Table 4 illustrates that these are rather complicated. While the flows on the ruptured faults (on the diagonal) have generally decreased from their linear Darcy-like responses at early times, they all remain higher than the pre-rupture flows. Moderate changes (a few×10%) in the flows on the 'non-ruptured' faults are the rule rather than the exception, most notably the reduction by 50% which occurs in the Maleme fault flow in response to a Whirinaki rupture. In this case however, there is little discernable effect in either the Ngakuru or Paeroa faults. The mixture of both increasing and decreasing surface flows (ratios above and below 1) suggests the effects of position within the graben (and perhaps relative to the heat source), fault permeability and connectivity with the other faults all play a role in determining the surface flows from each of the faults.

Finally, we note that at 100 years there is no case where there is a reversal of any surface flow, i.e. a negative flow ratio indicating a change from a pre-rupture downflow to a post-rupture upflow, or vice-versa. This suggests that an 'inertia' of flow exists within the graben which is difficult to change, even with relatively large perturbations of the fault permeabilities. Indeed, further modelling, not described here, suggests this to be the case – even arbitrarily large increases in fault permeabilities do not result in a flow reversal. This has the clear implication that the transient hydrothermal activity needed to create sinter deposits will not result from fault ruptures, at least not with the present model geometry and parameters.

Table 4: Summary of changes in flows at the ground surface, expressed as the ratio of the surface flow at the indicated time to the surface flow in the pre-rupture initial state. The largest ratios (yellow cells) occur on the diagonal elements of the table and pertain directly to the ruptured faults. The green cells indicate flow changes of >10%, and non-highlighted entries occur when there has been < 10% flow change.

	Ngakuru flow ratio		Maleme flow ratio		Whirinaki flow ratio		Paeroa flow ratio	
	0.001 yrs	100 yrs	0.001 yrs	100 yrs	0.001 yrs	100 yrs	0.001 yrs	100 yrs
Ngakuru rupture	**11.55**	**9.72**	1.00	0.71	1.00	0.76	1.00	1.03
Maleme rupture	1.00	0.87	**3.47**	**3.67**	1.00	1.00	1.00	1.36
Whirinaki rupture	1.00	0.99	1.00	0.50	**6.65**	**3.37**	1.00	1.02
Paeroa rupture	1.00	1.34	1.00	1.41	1.00	1.39	**3.05**	**1.90**

5.3 Effect of Fault Sealing

We now describe a series of models where each fault in turn has its permeability reduced to a 'background' level equal to the deep infill – 1 mD. Table 5 gives the flow ratios for these models. The format of the table is identical to that of Table 4. At 0.001 years, the flow ratios in all of the non-sealed faults show no change, while those in the sealed faults (yellow cells) have been reduced to ~1% of their initial levels. The reason for this is exactly the same as that for the early-time behaviour following the fault ruptures – the response in the sealed faults is linear (and in proportion to the permeability changes), and for the non-sealed faults there has not yet been enough time for pressure transmission through the faults system to produce an appreciable change elsewhere.

At 100 years the flow ratios in the sealed faults remain low, while the response elsewhere in the graben is generally more extreme than those in section 4.2, where the faults were ruptured. The smallest impact occurs on the sealing of the Ngakuru fault, with the changes (actually increases) in flow induced in the Maleme and Whirinaki faults being ~10% at most. Recalling that these faults both host downflows of water from the surface in the initial, pre-sealing state, these increases can be interpreted as partly compensating for the loss of fluid transfer which occurred from the Ngakuru to the Whirinaki when the Ngakuru fault was sealed. The small flow in the initial state and the relatively small response to its rupturing both suggest that the Ngakuru fault plays only a minor role in the regional hydrology. The results here reinforce this – evidently the Ngakuru fault's location on the western side of the graben and ~10 km distance from the heat source means that it is the least hydrologically active fault in the graben.

The sealing of the Maleme and Whirinaki faults produce effects of similar magnitude on the surface flows from the other faults. The Maleme and Whirinaki faults are both internal to the graben and provide the high-permeability west-east connectivity between Ngakuru and Paeroa. Sealing of either fault disrupts the graben-scale flows and causes, as the table shows, reductions in flow of between about 10% and 50% on both the Ngakuru and Paeroa faults. In the case of Maleme, the effects are slightly more extreme – the reduction in the Whirinaki flow ratio (to 0.22) is the largest in Table 5 (excepting the diagonal terms). Interestingly, although Maleme is the only fault directly connected to the Paeroa, the flow to the surface in the latter decreases by only 8% – not as much as might be expected given the removal of the (major) input it received (prior to Whirinaki sealing) from the Maleme at depth. Our modelling shows that the fluid required to maintain this high level of flow is sourced from newly created downflows just to the west (within 1-2 km) of the Paeroa fault. This fluid enters the Paeroa fault laterally from the west and (mostly) from within the permeable shallow infill.

The Paeroa fault, as we have seen, provides the most favoured conduit for outflowing fluid in the graben, and increasing the permeability of any of this or any of the other three major faults does not alter this fact. By contrast, the sealing of Paeroa fault results in the collapse of the flows to the surface on a graben-wide scale. Table 5 shows this; in the Whirinaki and Maleme faults the flows reduce to levels ~1%, and to 15% in the case of the Ngakuru fault. Thus, it seems that blocking the most preferred outflow path will have the greatest overall effect on the hydrological system. We see from the table that the surface flow hosted by the Maleme fault, while small, has actually reversed its direction, becoming an outflow where none previously existed. It thus provides the seed for new surface geothermal activity to occur within the Ngakuru Graben. In the absence of further changes in fault permeability our model shows that this outflow will continue to grow and eventually become the 'primary' outflow in the graben, with a magnitude similar to that of the initial pre-sealing flow on the Paeroa fault. Whether this outflow is then maintained, or is merely a transient hydrothermal 'event' will depend on the exact sequence and magnitudes of the fault permeability changes which follow.

Table 5: Summary of changes in flows at the ground surface, expressed as the ratio of the surface flow at the indicated time to the surface flow in the pre-sealing initial state. Positive flow ratios indicate the no change in flow direction has occurred, while negative ratios indicate a flow reversal. The largest ratios (yellow cells) occur on the diagonal elements of the table and pertain directly to the sealed faults. The green cells indicate flow changes of >10% and non-highlighted cells occur when there has been < 10% flow change.

	Ngakuru flow ratio		Maleme flow ratio		Whirinaki flow ratio		Paeroa flow ratio	
	0.001 yrs	100 yrs	0.001 yrs	100 yrs	0.001 yrs	100 yrs	0.001 yrs	100 yrs
Ngakuru sealing	**0.01**	**0.002**	1.00	1.12	1.00	1.11	1.00	0.99
Maleme sealing	1.00	0.55	**0.004**	**0.001**	1.00	0.22	1.00	0.62
Whirinaki sealing	1.00	0.63	1.00	0.72	**0.008**	**0.02**	1.00	0.92
Paeroa sealing	1.00	0.15	1.00	-0.03	1.00	0.02	**0.004**	**0.004**

6. DISCUSSION AND CONCLUSIONS

In this paper we have presented results from a TOUGH2 hydrological model of the Ngakuru Graben, in the Taupo Rift, New Zealand. The model extends to 7 km depth and incorporates a deep heat source to the south-east of the graben inferred from recent MT data. The model contains three major geological units (shallow/deep infill and a low-permeability unit exterior to the graben) and represents the four major faults (Ngakuru, Maleme, Whirinaki and Paeroa) within the graben as an interconnected series of permeable channels, ~150 m wide that penetrate to the base of the model. We establish the initial state for the model by choosing permeabilities for the faults which are proportional to their average slip rates, and this gives a state where a dominant upflow occurs on the Paeroa fault, with downflows on the Ngakuru, Maleme and Whirinaki faults. This is consistent with the fact that the Paeroa is historically the most active fault in the system.

We use this model to investigate the relationship between changes in the regional-scale hydrology caused by permeability transients in the faults and the presence of fossil sinters and other manifestations of past geothermal activity in the graben. To do this, we subject each of the faults, in turn, to instantaneous 'rupture' or 'sealing' by enhancing or reducing the permeability and then evolve the model for a period of 100 years. Upon rupture, the fault permeabilities are increased to 1000 mD, a level high enough to significantly affect all of the surface inflows/outflow across the graben on this timescale. Conversely, on sealing the fault permeabilities are reduced to 1 mD, equal to that of the 'deep infill' in the model and so effectively causing the faults to disappear.

Rupturing of any of the faults produces an immediate effect in that fault – the flow at the surface, whether up or down, changes in direct proportion to the ratio of the post-rupture to pre-rupture permeabilities. This is to be expected as the modelling assumes Darcy's law, where the flow rate is linearly dependent on the permeability. We take no account of any poro-elastic effects in modelling the consequences of fault rupture (cf. Dempsey et al., 2013). At later times, between 1 to 10 years, interaction between the faults and the surrounding formation is established graben-wide and the surface flows readjust to levels that are rather subdued with respect to the initial linear response. While our assumptions are quite different to the models of Dempsey et al. (2013) for the Te Kopia system, like them we find that fault ruptures, as simulated by increasing fault permeability, affect surface fluid flows; however we find that elevated flowrates persist for periods of at least 100 years.

The process of rupturing means that the fault permeabilities all remain relatively high, so the fault system as a whole remains well connected across the graben. A consequence of this is that rapid, diffusive, propagation of pressure signals through the fault system is always possible, and this explains the rapid cross-graben responses in surface flows that we noted above. An unexpected result of these models is that that we do not see the creation of new surface flows following the rupture of any of the faults. Thus, rupturing on any fault does not seem able to explain the presence of past transient hydrothermal activity elsewhere in the graben. Of course, ruptures on any of the faults do cause changes in the surface flow at the Paeroa fault, and can perhaps explain the high level of activity on that fault at different times.

In contrast to this, in models where the faults become sealed we find generally greater responses in the surface flows. Although the same rapid linear response is observed in these flows at early times, the lack of connectedness between the faults means that the longer time responses are quite different and indeed quite extreme in some cases. While sealing of the Ngakuru fault has only a modest effect on the other surface flows, sealing of the Paeroa fault results in the almost complete collapse of all the surface flows in the graben. It also produces the only new upflow (in the Maleme fault) we have seen in our models so far. The collapse of the flows in the Ngakuru, Maleme and Whirinaki faults is presumably related to their being largely isolated, hydrologically speaking, from the heat source following the sealing of the Paeroa fault. In spite this isolation, the deep penetration of the Maleme fault to a region where there is still a significant heat source may be the reason for the small upflow which appears there.

In conclusion, we have found that fault sealing is able to produce new outflows within the graben whereas this does not seem to be possible following fault ruptures. Thus fault sealing is the more likely cause of the past transient geothermal activity we see evidence for in the Ngakuru graben. We caution that this result applies strictly only to the particular model presented here. Clearly even this simple model behaves in a complicated manner and the presence or otherwise of transient upflows which can leave deposits of geothermal minerals at the surface depends (at least) on the fault and graben geometry, the permeabilities of all geological units and the location of the heat source. The general behaviour of systems of this type is far from being understood, and will be the subject of further work.

REFERENCES

Acocella, V., Spinks, K., Cole, J., & Nicol, A. Oblique back arc rifting of Taupo Volcanic zone, New Zealand. *Tectonics*, **22(4),** (2003).

Berryman, Kelvin, Pilar Villamor, Ian Nairn, Russ Van Dissen, John Begg, and Julie Lee.: Late Pleistocene surface rupture history of the Paeroa fault, Taupo rift, New Zealand. *New Zealand Journal of Geology and Geophysics*, **51/2**, (2008): 135-158.

Bertrand, E.A., Caldwell, T.G., Hill, G.J., Wallin, E.L., Bennie, S.L., Cozens, N., Onacha, S.A., Ryan, G.A., Zaino, A., and Wameyo, P.. Magnetotelluric imaging of upper-crustal convection plumes beneath the Taupo Volcanic Zone, New Zealand. *Geophysical Research Letters*, **39**, (2012), L02304 doi:10.1029/2011GL050177.

Bibby, H.M., Caldwell, T.G., Davey, F.J. and Webb, T.H.: Geophysical evidence on the structure of the Taupo Volcanic Zone and its hydrothermal circulation. *Journal of Volcanology and Geothermal Res*earch **68**, (1995), 29-58.

Brathwaite, R.L.: Geological and mineralogical characterization of zeolites in lacustrine tuffs, Ngakuru, Taupo Volcanic Zone, New Zealand. *Clays and Clay Minerals,* **51**, (2003) 589-598.

Bryan, C.J., Sherburn, S., Bibby, H.M., Bannister, S.C.: Shallow seismicity of the central Taupo Volcanic Zone, New Zealand: its distribution and nature. *New Zealand Journal of Geology and Geophysics*, **42**, (1999), 533-542.

Canora-Catalán, Carolina, et al.: Rupture history of the Whirinaki Fault, an active normal fault in the Taupo Rift, New Zealand. *New Zealand Journal of Geology and Geophysics*, **51.4**, (2008): 277-293.

Dempsey, D.E., Archer, R.A., Ellis, S.M., Rowland, J.V.: Hydrological effects of dip-slip fault rupture on a hydrothermal plume. *Journal of Geophysical Research*, **118**, (2013), 195-211, doi:10.1029/2012JB009395.

Gravley, D.M., Wilson, C.J.N., Leonard, G.S. and Cole, J.W.: Double trouble: paired ignimbrite eruptions and collateral subsidence in the Taupo Volcanic Zone, New Zealand. *GSA Bulletin*, **119**, (2007), 18-30.

Haar, L., Gallagher, J.S., Kell, G.S.: NBS/NRC Steam Tables, 320 pp. Hemisphere Publishing, New York (1984).

Heise, W., Caldwell, T.G., Bibby, H.M, and Bennie, S.L.: Three- dimensional electrical resistivity image of magma beneath an active continental rift, Taupo Volcanic Zone, New Zealand. *Geophysical Research Letters*, **37**, (2010), L10301. doi:10.1029/2010GK043110.

Houghton, B.F., Wilson, C.J.N., McWilliams, M.O., Lanphere, M.A., Weaver, S.D. and Briggs, R.M., Pringle, M.S.: Chronology and dynamics of a large magmatic system, central Taupo Volcanic Zone, New Zealand. *Geology,* **21**, (1995), 13-16.

Ingebritsen, S.E. and Manning, C.E.: Permeability of the continental crust: dynamic variations inferred from seismicity and metamorphism. *Geofluids,* **10**, (2010), 193-205.

Kissling, W.M.: Extending MULKOM to super-critical temperatures and pressures. *Proceedings.* World Geothermal Congress, Florence, Italy, (1995), 1687 – 1690.

Kissling, W.M. and Weir, G.J.: The Spatial Distribution of the Geothermal Fields in the Taupo Volcanic Zone, New Zealand. *J. Journal of Volcanology and Geothermal Res*earch, **145,** (2005), 136-150.

Kissling, W.M., Ellis, S., Charpentier, F., Bibby, H.M.: Convective flows in a TVZ-like setting with a brittle/Ductile transition. *Transport in Porous Media*, **77**, (2009), 335-355.

Litchfield, N. J., R. Van Dissen, R. Sutherland, P. M. Barnes, S. C. Cox, R. Norris, R. J. Beavan et al.: A model of active faulting in New Zealand. *New Zealand Journal of Geology and Geophysics*, (2014), 1-25.

Leonard, G.S., Begg, J.G. and Wilson, C.J.N. (compilers): Geology of the Rotorua Area. *Inst. of Geol. & Nucl. Sci.* 1:250 000 geological map 5. 1 sheet + 102 p. Lower Hutt, New Zealand. GNS Science (2010).

Matsushima, Jun, and Yasukuni Okubo.: Rheological implications of the strong seismic reflector in the Kakkonda geothermal field, Japan. *Tectonophysics*, **371.1,** (2003): 141-152.

Pruess, K.: TOUGH2 – A General Purpose Numerical Simulator for Multi-phase Fluid and Heat Flow. Report LBL-29400. Lawrence Berkeley Laboratory, 70pp (1991).

Rowland, J.V. and Sibson, R.H.: Extensional kinematics within the Taupo Volcanic Zone, New Zealand: soft-linked segmentation of a continental rift system. *New Zealand Journal of Geology and Geophysics*, **44**, (2001), 271-283.

Stagpoole, V.M. and Bibby, H.M.: Electrical resistivity map of the Taupo Volcanic, New Zealand; nominal array spacing 500 m, 1:250 000, version 1.0. Institute of Geological & Nuclear Sciences geophysical map 11. Institute of Geological & Nuclear Sciences Ltd., Lower Hutt, N.Z. (1998).

Stirling, M., McVerry, G., Gerstenberger, M., Litchfield, N., Van Dissen, R., Berryman, K., Jacobs, K.: National seismic hazard model for New Zealand: 2010 update. *Bulletin of the Seismological Society of America*, **102(4),** (2012), 1514-1542.

Villamor, P. and Berryman, K.: A late Quaternary extension rate in the Taupo Volcanic Zone, New Zealand, derived from fault slip data. *New Zealand Journal of Geology and Geophysics*, **44**, (2001), 243-269.

Wallace, L. M., Beavan, J., McCaffrey, R., & Darby, D. (2004). Subduction zone coupling and tectonic block rotations in the North Island, New Zealand. *Journal of Geophysical Research: Solid Earth*, (1978–2012), 109(B12).

Wilson, C.J.N., Houghton, B.F. and Lloyd, E.F.: Volcanic history and evolution of the Maroa-Taupo area, central North Island. *In* Smith, I.E.M. *ed*. Late Cenozoic volcanism in New Zealand. *Royal Society of N.Z. Bulletin.* **23**, (1986), 194-223.

Wilson, C.J.N., Houghton, B.F., Lanphere, M.A. and Weaver, S.D.: A new radiometric age estimate for the Rotoehu Ash from Mayor Island volcano, New Zealand. *New Zealand Journal of Geology and Geophysics*, **35**, (1992), 371-374.

Wilson, C.J.N., Houghton, B.F., McWilliams, M.O., Lanphere, M.A., Weaver, S.D., & Briggs, R.M.: Volcanic and structural evolution of Taupo Volcanic Zone, New Zealand: a review. *Journal of Volcanology and Geothermal Research*, **68(1),** (1995),1-28.